



## Characterization and simulation of transverse noise waves of a Multi-sensor solid streamer

Viktor Smirnov, Anthony Sourice, Julien Ribette, Jerome I. Mars, Philippe Herrmann

### ► To cite this version:

Viktor Smirnov, Anthony Sourice, Julien Ribette, Jerome I. Mars, Philippe Herrmann. Characterization and simulation of transverse noise waves of a Multi-sensor solid streamer. SEG/AAPG International Meeting for Applied Geoscience & Energy, Aug 2022, Houston, United States. 10.1190/image2022-3746522.1 . hal-03876640

**HAL Id: hal-03876640**

**<https://hal.science/hal-03876640>**

Submitted on 28 Nov 2022

**HAL** is a multi-disciplinary open access archive for the deposit and dissemination of scientific research documents, whether they are published or not. The documents may come from teaching and research institutions in France or abroad, or from public or private research centers.

L'archive ouverte pluridisciplinaire **HAL**, est destinée au dépôt et à la diffusion de documents scientifiques de niveau recherche, publiés ou non, émanant des établissements d'enseignement et de recherche français ou étrangers, des laboratoires publics ou privés.

# Characterization and simulation of transverse noise waves of a Multi-sensor solid streamer

Viktor Smirnov\* (Sercel / Univ. Grenoble-Alpes, GIPSA-Lab), A. Sourice (Sercel), J. Ribette (Sercel), J. Mars (Univ. Grenoble-Alpes, GIPSA-Lab), P. Herrmann (Sercel)

## Summary

Multi-sensor streamers have many advantages over traditional hydrophone-only streamers. In particular, they provide a measure of the pressure gradient which allows for data driven only broadband de-ghosting. This results in an improved subsurface image and allow the streamer to be towed deeper, reducing noise and operational downtime. However, the use of particle motion sensors is limited due to strong vibration noise waves they are subjected to.

In this article a detailed characterization of these waves is proposed. Reviewing the classical model of the propagation of transverse waves, a new model of their propagation velocity is obtained. This one allows to explain the velocity difference observed on field data between the waves that go down and up the streamer. A simple attenuation model is proposed to estimate their amplitude decay as they propagate along the streamer. Knowing these new characteristics, a simulation of these waves is performed that matches the real data with high accuracy.

## Introduction

Multi-sensor streamers with hydrophones and particle motion sensors have significant advantages over conventional streamers with hydrophones only, including:

- **Reconstruction of a broadband spectrum without prior.** The angle and frequency dependent reflection of the seismic wavefield at the water-air interface causes destructive interference in the hydrophone spectrum, classically called ghosts, which can strongly limit the resolution of the final subsurface image. By properly combining hydrophone components and particle motion sensors, it is possible to remove these ghosts [Tenghamn 2009]. Nowadays, multi-component streamers are the preferred acquisition solution [Goujon 2019] because they do not require prior knowledge on sea state, seismic wavelet shape nor geology in order to perform de-ghosting [Ozdemir 2012] while keeping the acquisition configuration and processing simple.
- **Reduced operation downtime, decreased swell noise and increased low frequency content by towing deeper.** Ghost removal allows for deeper towed streamer acquisitions. Thus, acquisitions are less dependent on weather conditions and swell noise is greatly reduced [Hlebnikov 2021] which allows for a reduction in technical downtime (1 % or less over two campaigns conducted in 2018 [Firth 2018]). The low-frequency

content is also increased (11 dB gain at 5 Hz for an acquisition at 40 m compared to 10 m [Firth 2014]) which reduces cycle-skipping in the Full-Waveform Inversion and allows quantitative improvement of the elastic inversion.

However, unlike hydrophones which by design are not sensitive to streamer vibration, particle motion sensors are strongly affected [Teigen 2012]. These waves mainly show modes transverse to the inline direction of the streamer and are mostly generated by positioning devices, lead-in and swell [Mellier 2014]. They travel at low velocities (<150 m/s) and are highly coherent in between two positioning devices (~150 m). These waves have very strong amplitudes (20 dB higher than seismic reflections at 10 Hz [Sanchis 2014]) and different techniques have been used to mitigate them. A first technique is to filter these waves based on their slowness [Ozdemir 2012] with a fine digital spatial sampling of 0.7 m [Goujon 2019] to avoid aliasing issues. Compared to conventional 12.5 m sampling, this requires a large increase in the number of sensors and additional power, resulting in a significant additional cost for the customer. Another technology is to keep a standard intertrace and use analog sensor arrays. This technology has proven to be successful in reducing transverse waves contamination above 20 Hz. The SNR can be further improved with some processing [Hlebnikov 2021], which allow not to depend on the short wavelength sea state in the de-ghosting process. Below 20 Hz, only hydrophones are used for de-ghosting because, to our knowledge, there is no filtering method that can significantly reduce the transverse waves unattenuated by the analog array [Sanchis 2014].

In this paper, a characterization of the velocity and attenuation of transverse waves will be performed. This will allow us to better understand the physics of these waves and to simulate them with great accuracy in order to be able to mitigate them in the future.

## Streamer transverse displacement and dispersion

The first model of the transverse displacement of the streamer was proposed by Teigen et al. [Teigen 2012]. The authors propose to use the Bernoulli Euler equation:

$$EI \frac{\partial^4 u(x,t)}{\partial x^4} - T \frac{\partial^2 u(x,t)}{\partial x^2} + \frac{\pi d^2 \rho_s}{4} \frac{\partial^2 u(x,t)}{\partial t^2} = f_m(x,t) + h(x,t) \quad (1)$$

where  $u(x,t)$  is the transverse displacement of the streamer,  $E$  the Young's modulus,  $I$  the area moment of inertia,  $T$  the axial tension,  $d$  the streamer diameter,  $\rho_s$  the streamer density,  $f_m(x,t)$  the inertial force and  $h(x,t)$  the external force per unit of length.

## Characterization and simulation of transverse noise waves

Considering that the inertial force corresponds only to the acceleration of the displaced fluid mass, i.e.  $f_m(x, t) = -\frac{\pi d^2 \rho_w}{4} \frac{\partial^2 u(x, t)}{\partial t^2}$  where  $\rho_w$  is the density of the water, and no external forces, the authors obtain the following phase velocity:

$$v_p(k) \equiv \frac{f(k)}{k} = \pm \frac{2}{d} \sqrt{\frac{4\pi^2 k^2 E I + T}{\pi(\rho_s + \rho_w)}} \quad (2)$$

This relationship correctly reflects the dispersive nature of the transverse wave velocity that is observed in the field data [Teigen 2012][Sanchis 2014]. However, it does not explain the velocity difference observed between Downgoing transverse Waves (DW) which travel from the streamer head to the tail and Upgoing transverse Waves (UpW) which travel from the streamer tail to the head. To take into account this difference, Berera proposes to add two terms to the inertial force that represents the virtual mass due to the streamer tow [Berera 2004], the new expression is:

$$f_m(x, t) = -\frac{\pi d^2 \rho_w}{4} \left( \frac{\partial^2 u(x, t)}{\partial t^2} + U_0^2 \frac{\partial^2 u(x, t)}{\partial x^2} + 2U_0 \frac{\partial^2 u(x, t)}{\partial t \partial x} \right) \quad (3)$$

where  $U_0$  is the water-speed, i.e. the speed of the streamer relative to the water. A new expression for the velocity of transverse waves is then obtained:

$$v_p(k) \equiv \frac{f(k)}{k} = -\frac{U_0}{2} \pm \frac{2}{d} \sqrt{\frac{4\pi^2 k^2 E I + T - \frac{\pi(\rho_s + \rho_w) d^2 U_0^2}{16}}{\pi(\rho_s + \rho_w)}} \quad (4)$$

Firstly this expression shows that the velocity difference between DW and UPW is constant over the whole frequency band and equal to the water-speed. Secondly, it introduces a corrective tension term ( $\frac{\pi(\rho_s + \rho_w) d^2 U_0^2}{16}$ ) that can be neglected

because it is less than 10 N compared to tensions of several kN for conventional seismic acquisitions.

Figure 1 shows a comparison of the transverse velocity model proposed by Teigen and the new model introduced in this paper. On the top panel, these two models are plotted as a function of frequency for a tension of 16.4 kN and a water-speed of 2 m/s, the dispersive nature of transverse waves can be observed (high frequencies move faster than low frequencies). As stated above and according to equation (4), a constant velocity difference over the entire frequency band and equal to half the water velocity between the two models is observed. The bottom panel shows an FK representation of field data overlaid with the velocity models shown in the top panel. The data are particle motion sensor records from a seismic-free sequence (noise only), the FK is calculated for Reception Points 13 to 26 over a 240 s window. This FK shows that the transverse waves are the dominant noise. They are strongly aliased because of the 12.5 m inter-trace and the effect of the spatial group which strongly attenuates the transverse waves above about 25 Hz can also be seen. The velocity model for UPW is superimposed in white, the solid lines correspond to the Teigen model and the one proposed in this paper is drawn in dotted lines. The same conventions are adopted for the DW drawn in black. The difference between the models is noticeable from about 15 Hz and it can be seen that Teigen's model slightly overestimates the velocity of the UpW and underestimates the velocity of the DW. By taking into account the water-speed, a difference in velocity between the upgoing and downgoing waves is introduced, allowing the proposed model to provide a better regression of the data.

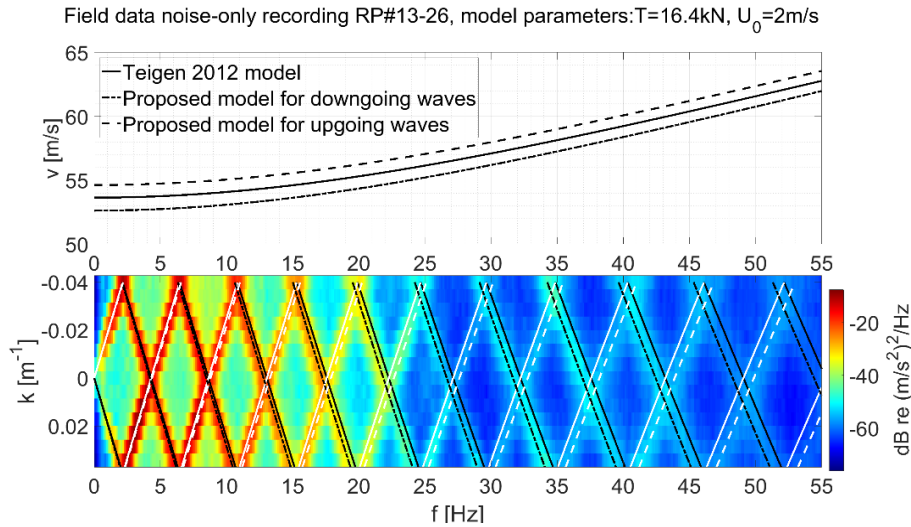


Figure 1: (Top) Transverse wave velocity as a function of frequency  $f$ , for a tension  $T=16.4$  kN and a water-speed  $U_0=2$  m/s. The solid line curve corresponds to the dispersive model presented by Teigen (eq. 2), those in dotted lines correspond to the dispersive model (eq. 4). (Bottom) FK representation of field data particles motion sensors RP#13-26 (noise-only recording) and overlay of the velocity models presented above. The black dotted lines correspond to the UPW velocities and the white dotted ones to the DW (eq. 4), the solid lines are Teigen model eq. 2.

## Characterization and simulation of transverse noise waves

After introducing a new velocity model we focus on attenuation characteristics.

### Attenuation

To the authors' knowledge, the attenuation of transverse waves during their propagation along the streamer has never been described in the literature. In this paper, a simple model is proposed to determine this attenuation based on the following physical and practical assumptions:

- Particle motion sensor data record only transverse wave noise during acquisition without a seismic signal
- Positioning devices are the only sources generating transverse waves
- Positioning devices emit upgoing and downgoing transverse waves with equal energy
- Transverse waves propagate with attenuation described by  $e^{-\alpha \cdot d}$ , where  $d$  is the distance traveled by the wave along the inline axis of the streamer and  $\alpha$  is the attenuation coefficient in  $m^{-1}$
- Positioning devices perfectly attenuate the incident transverse waves

With these assumptions, it is possible to perform a non-linear regression that explains the RMS value of the particle motion data from a coefficient  $\alpha$  and the RMS values emitted by each source to be determined. Figure 2 shows this regression performed on field data from a noise-only sequence of a seismic survey. The data have been filtered in the [2-20] Hz band where transverse waves are highly predominant. The RMS value of the data to fit is plotted in black, the RMS value obtained by regression is drawn in red. As can be seen in the figure, the regression provides a very

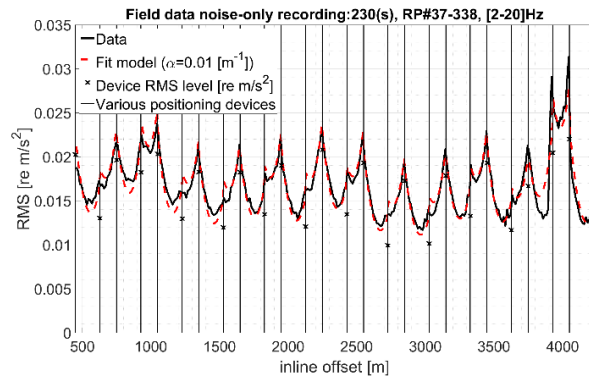


Figure 2: RMS value as a function of the streamer's inline position. The vertical lines correspond to the positioning devices. RMS value of the particle motion sensors (band [2-20] Hz) is shown in black. Red dotted lines is obtained for an attenuation coefficient  $\alpha = 0.01 m^{-1}$  and the RMS values emitted by each device represented by the crosses.

good explanation of the data and results in an attenuation coefficient equal to  $\alpha = 0.01 m^{-1}$ .

From the new velocity model and knowing the attenuation of transverse waves a simulation is proposed.

### Simulation

This simulation consists of two steps: the modeling of the transverse wavelet generated by the noise sources and its propagation along the streamer.

Figure 3 illustrates how the transverse wave modeling is performed. We first create a colored noise with a Gaussian amplitude distribution whose Power Spectral Density (PSD) is represented in blue. This signal is then filtered by the analog array (PSD represented in green) and finally by the analog and digital filters specific to the streamer (red curve). The modeling thus performed accurately captures the behavior of the transverse wave since the final PSD (red) is close to the field data PSD plotted in black. The modeling of the transverse signal is carried out thanks to the knowledge of the various filters of the streamer studied and thus allows to easily simulate various acquisition configurations.

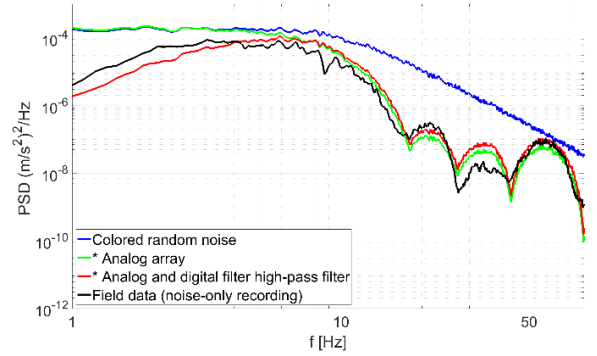


Figure 3: Power Spectral Densities (PSD) of transverse wave modeling and PSD of field data.

The resulting wave is propagated considering an attenuation coefficient of  $\alpha = 0.01 m^{-1}$  and the velocity of the downgoing wave (eq. 4), a simulation of DW is then obtained. From a new random draw of the wavelet and using the propagation velocity of the upgoing wave, a simulation of the UpW is obtained.

Figure 4 shows the result of this simulation in the  $[x, t]$  domain. The two left panels correspond to the DW and UpW, the right panels show the final result of the simulation (sum of DW & UpW) and a representation of field data (same configuration as used for the previous figures). These

## Characterization and simulation of transverse noise waves

field data and the simulation result with a small amount of additional Gaussian noise are plotted in the FK domain in Figure 5.

As can be seen in these two figures, the simulation matches the field data with a high quality in the [0-20] Hz band where transverse waves are predominant. As can be seen in figure 4, the interference between the DW and UpW creates complex patterns that are well captured by the simulation. Above 20 Hz (fig. 5) the simulation is less realistic but still very good. In particular, the velocity of transverse waves is well understood. To improve the model, the variations of attenuation and velocity of transverse waves in time and space still need to be studied.

### Conclusions

In this paper, a new transverse wave velocity model has been proposed. It allows to explain the velocity difference between the transverse waves going down (DW) the streamer and the one going up the streamer (UpW) and thus, fits the field data with a better quality than the existing models. A simple attenuation model has also been proposed which allowed to estimate the attenuation of these waves at  $0.01 \text{ m}^{-1}$ . With these new features, a high quality simulation of transverse waves has been achieved.

Transverse waves are the dominant noise of multi-sensor streamers which have significant advantages over

conventional ones. By improving our physical knowledge of these waves and by succeeding in simulating them, we believe that we will be able to provide tools to mitigate them more effectively in the future.

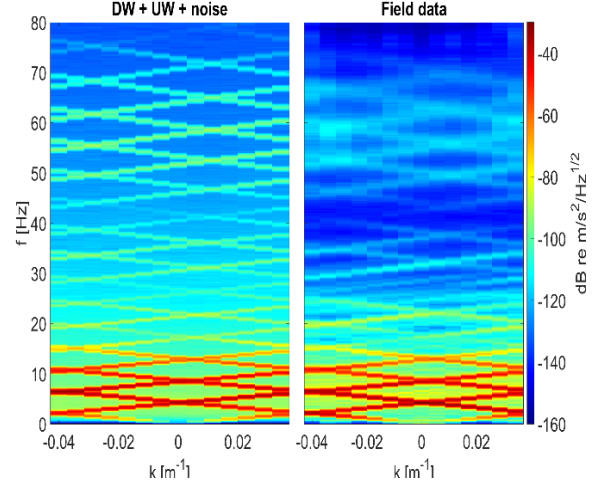


Figure 4: FK representation of the transverse waves. The left panel corresponds to the FK of the simulation result (DW & UpW) to which a slight Gaussian noise has been added. The right panel corresponds to the FK representation of the field data presented in figure 4.

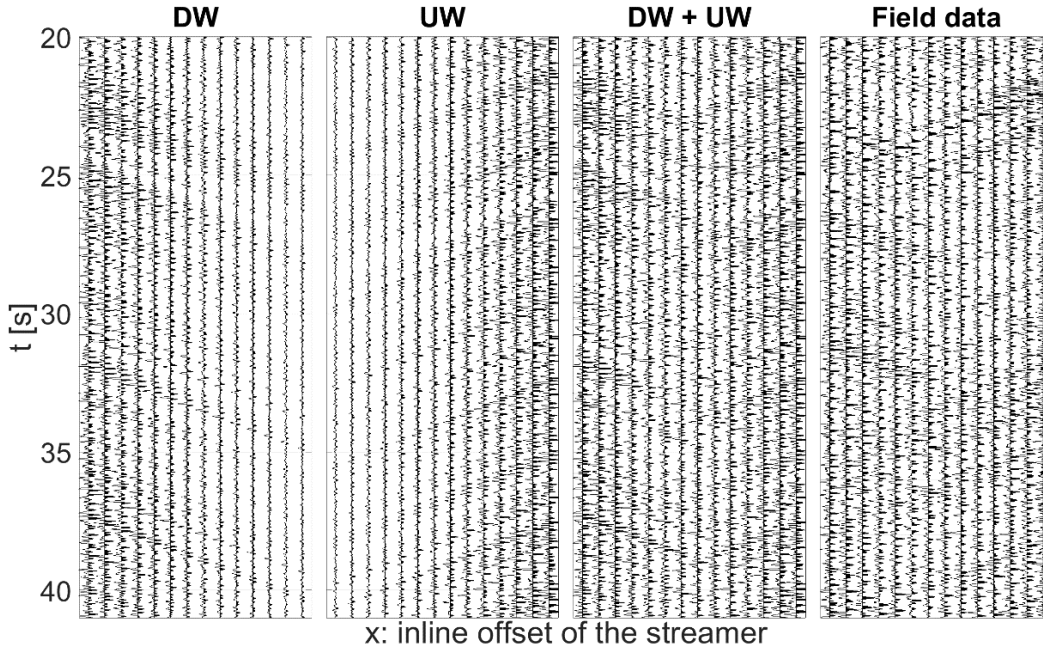


Figure 5: t-x representation of the transverse waves. From left to right : DW, UpW, sum of DW & UpW and field data respectively. A great similarity can be observed between the last two panels which shows the quality of the simulation.